



Tyrosine-sulfate isosteres of CCR5 N-terminus as tools for studying HIV-1 entry

Son N. Lam^a, Priyamvada Acharya^b, Richard Wyatt^b, Peter D. Kwong^b, Carole A. Bewley^{a,*}

^a Laboratory of Bioorganic Chemistry, National Institute of Diabetes, Digestive, and Kidney Diseases, National Institutes of Health, DHHS, Bethesda, MD 20892, USA

^b Vaccine Research Center, National Institute of Allergy and Infectious Diseases, National Institutes of Health, DHHS, Bethesda, MD 20892, USA

ARTICLE INFO

Article history:

Received 12 August 2008

Revised 1 October 2008

Accepted 1 October 2008

Available online 5 October 2008

Keywords:

HIV-1 gp120

Phenylmethanesulfonic acid

Tyrosine sulfonate

Saturation transfer difference NMR

Surface plasmon resonance

Enzyme-linked immunosorbent assay

Small molecule inhibitor

ABSTRACT

The HIV-1 co-receptor CCR5 possesses sulfo-tyrosine (TYS) residues at its N-terminus (Nt) that are required for binding HIV-1 gp120 and mediating viral entry. By using a 14-residue fragment of CCR5 Nt containing two TYS residues, we recently showed that CCR5 Nt binds gp120 through a conserved region specific for TYS moieties and suggested that this site may represent a target for inhibitors and probes of HIV-1 entry. As peptides containing sulfo-tyrosines are difficult to synthesize and handle due to limited stability of the sulfo-ester moiety, we have now incorporated TYS isosteres into CCR5 Nt analogs and assessed their binding to a complex of gp120–CD4 using saturation transfer difference (STD) NMR and surface plasmon resonance (SPR). STD enhancements for CCR5 Nt peptides containing tyrosine sulfonate (TYSN) in complex with gp120–CD4 were very similar to those observed for sulfated CCR5 Nt peptides indicating comparable modes of binding. STD enhancements for phosphotyrosine-containing CCR5 Nt analogs were greatly diminished consistent with earlier findings showing sulfo-tyrosine to be essential for CCR5 Nt binding to gp120. Tyrosine sulfonate-containing CCR5 peptides exhibited reduced water solubility, limiting their use in assay and probe development. To improve solubility, we designed, synthesized, and incorporated in CCR5 Nt peptide analogs an orthogonally functionalized azido *tris*(ethylenoxy) *L*-alanine (*L*-ate-Ala) residue. Through NMR and SPR experiments, we show a 19-residue TYSN-containing peptide to be a functional, hydrolytically stable CCR5 Nt isostere that was in turn used to develop both SPR-based and ELISA assays to screen for inhibitors of CCR5 binding to gp120–CD4.

Published by Elsevier Ltd.

1. Introduction

HIV-1 infection is initiated through interactions between the viral surface envelope (Env) glycoprotein gp120 and cellular receptors CD4 and CCR5 or CXCR4.^{1,2} CCR5 and CXCR4, also referred to as HIV-1 co-receptors, are 7-transmembrane spanning G-protein coupled receptors that have the unusual feature of containing sulfo-tyrosine (TYS) residues in their extracellular N-terminal domains.³ CCR5 N-terminus (Nt) contains four tyrosine residues at positions 3, 10, 14, and 15, and sulfation of at least residues 10 and 14 is essential for mediating viral entry.⁴ Moreover, CCR5 Nt peptides containing sulfo-tyrosine residues at positions 10 and 14 inhibit HIV-1 membrane fusion.^{5,6} Recently we showed by NMR that a CCR5 Nt peptide comprising residues 2–15 (**1**, Nt^{2–15}), where Tyr10 and Tyr14 are sulfated, binds CD4-activated HIV-1 gp120 (CD4–gp120) but not gp120 or CD4 alone; and that residues 9–15 adopt an ordered, alpha helical structure upon binding.⁷ Molecular docking of the minimized mean structure showed CCR5 Nt to dock in a single orientation to a conserved region on gp120 specific for sulfo-tyrosine. Those studies demonstrated that a CCR5 Nt peptide fragment can function as a natural co-receptor mimic.

Despite interesting and important biological roles, Tyr(SO₄)-containing peptides are not without liabilities. The ArO–SO₃[−] bond is prone to hydrolysis.⁸ Lack of robust protecting groups orthogonal to the sulfate group combined with the need for acid catalyzed cleavage of side chain protecting groups and peptide from resin can make peptide synthesis difficult and yields low. Furthermore, the need to prevent hydrolysis during chromatographic separations can make purification of crude peptides a challenge. Together, these factors place limitations on the use of Tyr(SO₄)-containing peptides as versatile biochemical probes and tools. We thus sought to develop a functional, non-hydrolyzable CCR5 Nt peptide analog amenable to orthogonal modifications and whose synthesis can be scaled up for assay development. To this end, we used saturation transfer difference⁹ (STD) NMR and/or surface plasmon resonance (SPR) techniques to investigate the effects on gp120 binding of CCR5 Nt peptides where (i) sulfo-tyrosine (referred to hereafter as TYS) residues were replaced by tyrosine phosphate [Tyr(PO₃^{2−}), referred to as TYP] and tyrosine sulfonate [Tyr(CH₂SO₃[−]), referred to as TYSN] isosteres (Fig. 1); (ii) their length was increased to 17 or 19 residues; (iii) a third TYS or TYSN isostere at residue Tyr3 was incorporated; and/or (iv) a C-terminal biotinylated polyethylene glycol linker was introduced. On the basis of these results, we have synthesized a functional CCR5 Nt analog (**8**) bearing chemically stable TYSN residues, and shown that

* Corresponding author. Tel.: +1 301 594 5187; fax: +1 301 402 4182.

E-mail address: caroleb@mail.nih.gov (C.A. Bewley).

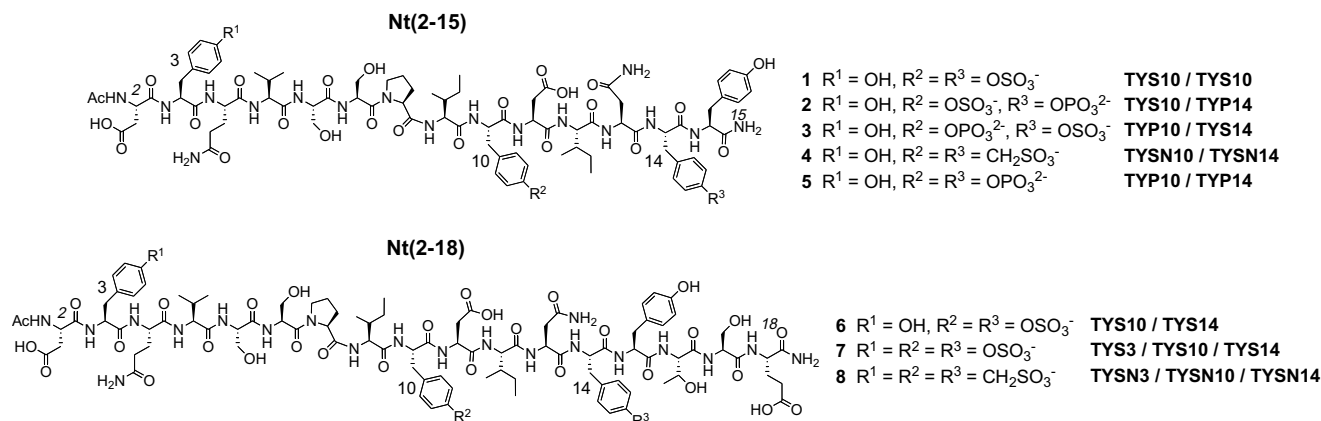


Figure 1. CCR5 Nt peptides and analogs.

when biotinylated through a PEG linker (**12**) the TYSN-containing construct can be used to screen in both SPR-based and ELISA platforms for molecules that specifically inhibit CCR5 Nt binding to HIV-1 gp120. Additionally, STD NMR of peptides containing one TYS and one TYP residue validate our model of CCR5 Nt binding to gp120.

2. Results and discussion

Recently we solved by NMR the solution structure of a functional 14-residue CCR5 Nt peptide comprising residues 2–15 (**1**) in complex with gp120–CD4.⁷ When bound to this complex, the backbone of residues 9–15 adopt an alpha helical structure that displays TYS10 and TYS14 from the same face of the helix (Fig. 2). Molecular docking of CCR5 Nt to the crystal structure of gp120–CD4 in complex with sulfated monoclonal antibody 412d showed Nt to bind to the base of the third variable loop (V3) in a manner similar to that of 412d. In the model, the side chain of TYS14 makes numerous hydrogen bonds and extensive van der Waal's interactions with positively charged and hydrophobic residues forming this site (Fig. 2, orange surface), and Tyr15 packs closely to several neighboring hydrophobic residues (Fig. 2, green surface). The side chain of TYS10 on the other hand is positioned further from gp120, possibly making hydrogen bonds through its sulfate group (Fig. 2, blue surface). This model was validated by STD NMR, a technique that gives rise to a difference spectrum whose proton signal intensities are proportional to their proximity to receptor.⁹ As seen in the expansion of the aromatic region of a 1D ¹H-STD NMR spectrum of **1** binding to gp120–CD4 (Fig. 3a), resonances corresponding to H_δ and H_ε of TYS14, and Tyr15, respec-

tively, exhibited the strongest enhancements within the entire spectrum (normalized to 100%), while those for TYS10 were estimated at ~66% (spectral overlap occurs between TYS10 H_δ and TYS10 H_ε), consistent with our docked model. Relative to these aromatic protons, enhancements for all other residues, including Tyr3, were negligible in comparison.

Having mapped by STD NMR the epitope used by CCR5-Nt to bind gp120, we next assessed binding to gp120–CD4 of Nt²⁻¹⁵ peptides bearing a single substitution of TYP in place of TYS at either position 10 or 14. As seen in the expansion of the aromatic region of the STD NMR spectrum for analog **2** which contains phosphotyrosine at residue 14, STD enhancements for TYP14 H_δ and H_ε decrease from 100% in **1** to 45% and 54% in **2**, respectively (Fig. 3b, Table 1). Enhancements for Tyr3 and Tyr15 were unaffected by the presence of TYP14, while enhancements for TYS10 increased slightly from 66% in **1** to 88% in **2**. In contrast, relative enhancements observed for tyrosine residues in analog **3** (Fig. 3c) containing TYP at position 10 and TYS at position 14 were more similar to those of **1** (Fig. 3a) with strongest enhancements observed for TYS14 and Tyr15 followed by TYP10. Although overlap between signals for Tyr3 H_δ and TYP10 H_ε, and TYP10 H_ε and TYP10 H_δ prevented accurate integration of the difference spectrum for **3**, a moderate decrease in intensity for signals corresponding to TYP10 H_δ and H_ε relative to the same atoms in **1** is apparent from comparison of Figure 3c with 3a. Incorporation of two TYP residues at positions 10 and 14 (**5**) resulted in complete loss of binding to gp120–CD4 (data not shown), in agreement with previous studies.⁴ Together, these results indicate that the Tyr14 binding site on CD4-activated gp120 has a strong preference for TYS while that of Tyr10 is less stringent and will accommodate phosphotyrosine, albeit with diminished interactions.

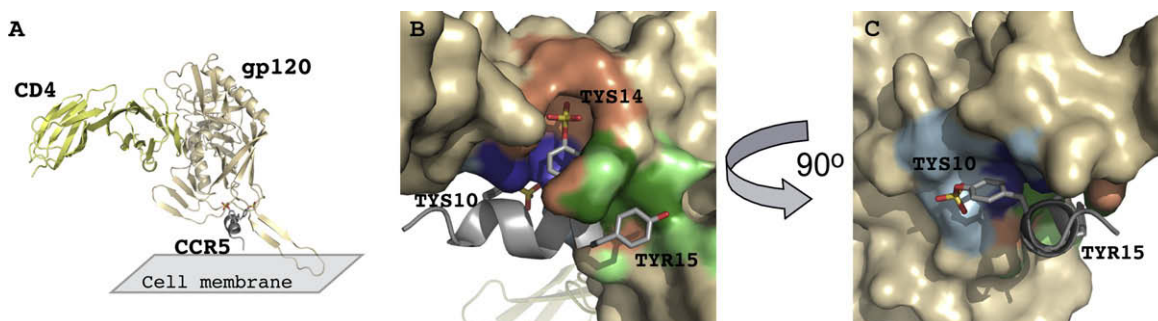


Figure 2. gp120–CCR5 interactions. (A) Model of CCR5 Nt (gray) docked to gp120 (beige)–CD4 (yellow). (B and C) Close-up of CCR5 Nt binding surface with gp120 rendered as a surface, and CCR5 Nt backbone a cartoon. Side chains of TYS10, TYS14, and Tyr15 (labeled) are drawn as sticks. In (C), the structure is rotated 90° about the z axis relative to (B). Contact surfaces unique to and within 5 Å of TYS10, TYS14 and TYR15 are colored light blue, orange, and green, respectively. Contact surfaces that overlap between TYS10 and TYS14 are colored dark blue, and surfaces that overlap between TYS14 and TYR15 are colored cyan.

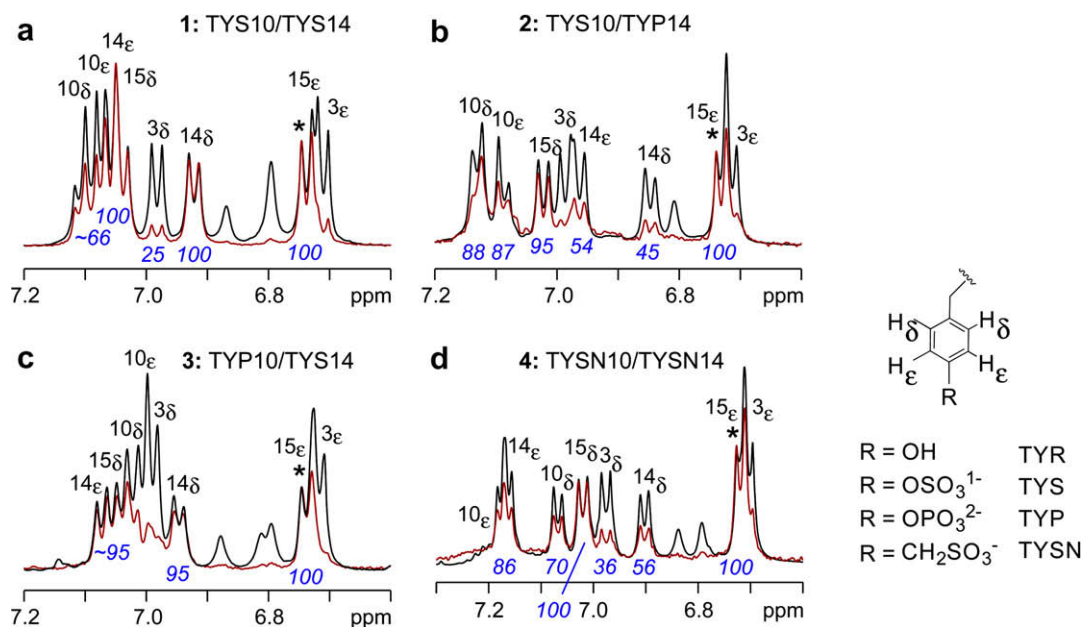


Figure 3. Aromatic region of ^1H STD NMR spectra of 14-residue CCR5 Nt $^{2-15}$ (**1**) and analogs **2–4**. Reference and difference spectra are shown in black and red, respectively. (a) CCR5 Nt $^{2-15}$ (**1**) containing TYS10 and TYS14; (b) analog **2** containing TYS10 and TYP14; and (c) analog **3** containing TYP10 and TYS14; (d) analog **4** containing TYSN10 and TYSN14. Spectra were recorded at 298 K on samples containing 20 μM gp120-CD4 in the presence of 800 μM peptide at pH 6.8 with spectra normalized to 15 ϵ (*).

Table 1
STD enhancements for peptides **1–4** binding to gp120-CD4^a

Peptide	10 δ	10 ϵ	14 δ	14 ϵ	15 δ	15 ϵ	Relative STD ^b
1	~70 ^c	~70 ^c	100	100	100	100	+++
2	88	87	45	54	95	100	+
3	^d	^d	95	95	95	100	+++
4	86	70	56	86	100	100	++

^a Aromatic proton resonances designated in bold. Enhancements for Tyr3 (not shown) ranged from 5% to 35% for peptides **1–4**.

^b STD enhancements of residue 14 relative to TYS in Nt $^{2-15}$ (**1**).

^c Integration is approximate due to overlap between these signals.

^d Overlap prevented integration; qualitative comparisons of spectra shown in Figure 3a and c indicate diminished enhancements relative to TYS10 in Figure 3b.

2.1. Sulfate versus sulfonate in the gp120 TYS binding pocket

At neutral pH, sulfo-tyrosine and phosphotyrosine bear formal charges of -1 and -2 , respectively. Although sulfate and phosphate groups differ slightly in size, because the Tys14 binding site on gp120 carries a single positive charge, we reasoned that the discrimination in binding sulfate versus phosphate might be attributed to this difference in charge.¹⁰ We next investigated the singly charged non-hydrolyzable phenylmethanesulfonic acid moiety Tyr-CH₂-SO₃⁻ (referred to as tyrosine sulfonate, or TYSN) as a TYS isostere.¹¹ Fmoc-protected tyrosine sulfonate was synthesized¹² and incorporated into CCR5 Nt analog **4**, and its binding to gp120-CD4 was assessed by NMR. The difference spectrum (Fig. 3d) for **4** in the presence of gp120-CD4 clearly indicated binding to the complex. In particular, enhancements for the aromatic protons of TYSN10 were comparable to those of TYS10 with values ranging from 70% to 86%, while slightly reduced binding of TYSN to the gp120 TYS14 binding site was apparent from an enhancement of 86% for H ϵ of TYSN14 relative to 100% for TYS14. On the other hand, direct comparison of values for both H δ and H ϵ of TYP versus TYSN reveals stronger enhancements for TYSN regardless of position. Providing further support that tyrosine sulfonate can act as a functional TYS isostere and bind in close proximity to gp120, strong STD enhancements also were observed for the methylene protons ($-\text{CH}_2-\text{SO}_3$) in both TYSN units.

A mode of binding of TYSN to gp120 that is similar to that of natural TYS and consistent with our NMR data is presented in Figure 4. CCR5 TYS14 binds in a deep pocket on gp120 containing several polar and one positively charged residue positioning the sulfate ester to make a full complement of hydrogen bonds with the side chains of Arg298, Asn302, and Thr303, and the backbone N atoms of Asn302, Thr303, and Gly441 (Fig. 4B). In the case of TYSN, the hydrogen bond between Asn302 and the ester oxygen would be lost, and steric clash between the sulfonate methylene and surrounding residues may be imposed (Fig. 4C). Any changes in the binding pocket resulting from these differences would be expected to reduce slightly the interactions with TYSN and gp120. Additionally, the presence of the single positive charge, provided by Arg298, may contribute to the selectivity of sulfate over phosphate.

2.2. Binding of CCR5 Nt(2–18) peptides

The predicted extracellular region of CCR5 N-terminus extends at least to residue 20, with Cys20 forming a disulfide bridge with Cys269 of the third extracellular loop and Tyr3 likely being sulfated.¹³ To examine the effects on binding gp120 longer CCR5 Nt peptides bearing two or three sulfo-tyrosine residues, samples comprising gp120-CD4 in complex with the 17-residue peptides **6** and **7**, where sulfo-tyrosines are present at positions 10/14 and 3/10/14, respectively, were prepared and investigated by NMR using conditions identical to those for **1–4**. Relative to 14-mer **1**, ^1H NMR spectra for both constructs showed increased line broadening in the presence of gp120-CD4, especially for TYS14 and Tyr15 (Fig. 5a and b; Table 2) suggesting that gp120 binds these constructs in slower exchange and with higher affinity than peptides **1–4**. ^1H STD NMR revealed strong enhancements for TYS10, TYS14, and Tyr15 in Nt $^{2-18}$ (**6**). Additionally, the γ -methyl of Thr16 showed appreciable STD enhancements (data not shown), while Tyr3 resonances did not. In triply sulfated CCR5 Nt peptide **7**, line broadening of H δ and H ϵ resonances of TYS14 and Tyr15 was even greater than in peptide **6** (Fig. 5b), suggesting the presence of TYS3 further stabilized the ternary complex of CD4-HIV-1 gp120-CCR5 Nt peptide and effectively reduced the peptide's off

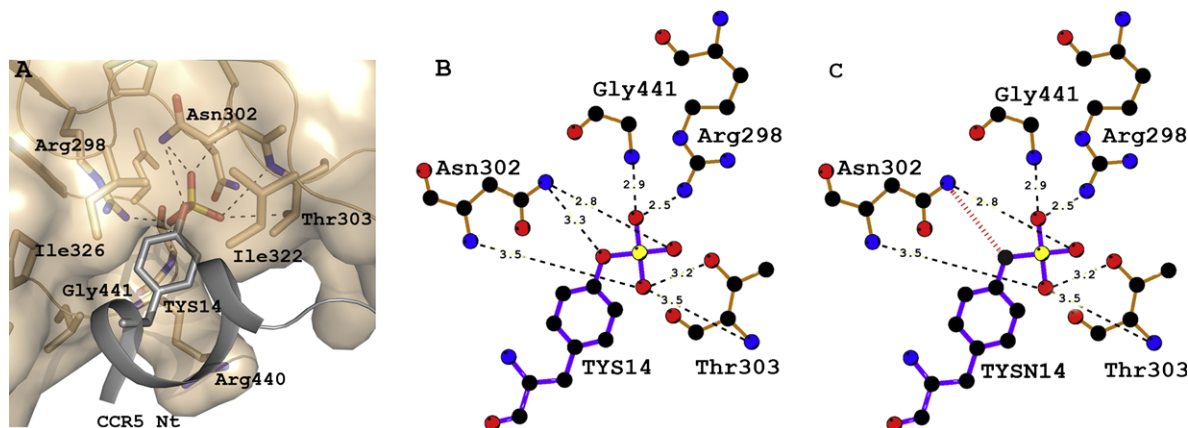


Figure 4. Comparison of TYIS and TYISN binding to gp120. (A) Close-up of TYIS-gp120 binding pocket with CCR5 Nt displayed as a gray ribbon; (B) hydrogen bonding network for TYIS binding to gp120; and (C) schematic showing potential differences in interactions between TYIS and TYISN binding to gp120, generated by simple atom replacement of CH₂ in TYISN for O in TYIS. Dashed red line indicates a potential clash between methylene of TYISN and the side chain amide of Asn302. Residue 14 shown in purple and gp120 residues in gold.

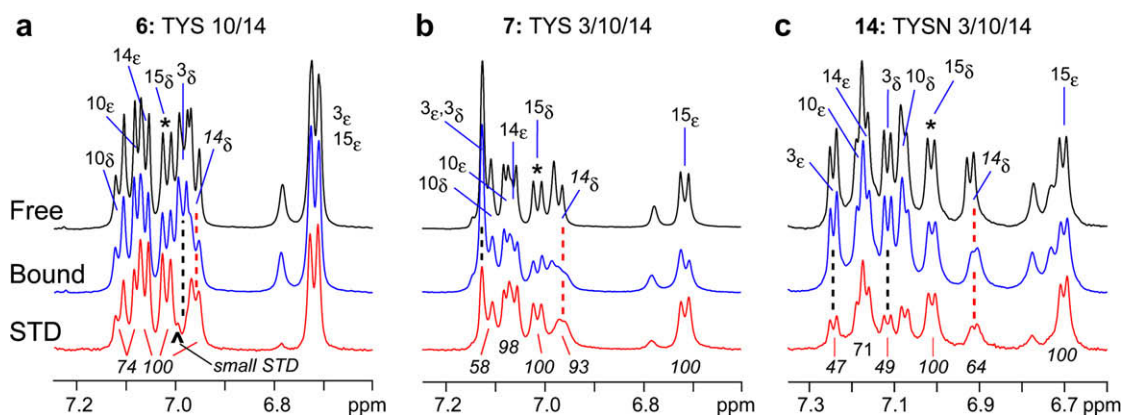


Figure 5. Expansions of NMR spectra of 17-residue CCR5 Nt (2–18) and analogs. ¹H NMR spectra of free and bound peptides are shown in black and blue, respectively, and ¹H STD spectra of complexes are red. Number and position of TYIS and TYISN residues are shown above respective spectra and in Figure 1 and in this figure.

Table 2

Increase in line width (Hz) between free and bound peptides^a

Peptide	10δ	10ε	14δ	14ε	15δ	15ε
1	1.0	— ^b	0.8	—	—	0.6
4	1.1	—	1.3	—	1.0	—
6	0.8	0.8	2.2	1.4	1.0	—
7	2.3	1.2	~3 ^c	2.8	2.9	2.8
14	2.4	—	2.8	—	1.9	3.2

^a NMR solutions contained 40:1 peptide/gp120-CD4.

^b Overlapped signals not measured.

^c Conservative estimate due to slight overlap between 14δ and side chain amide with severe line broadening apparent in Fig. 5b, blue spectrum.

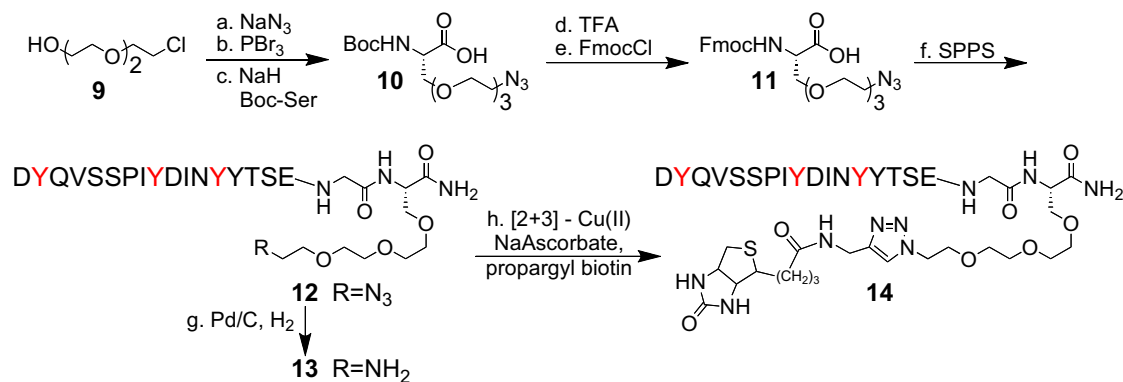
rate from complex. Overlap of several Hδ and Hε peaks of TYIS3 and TYIS10 prevented quantitative measure of STD enhancements for these residues. However, measurement of line widths in ¹H spectra of free versus bound peptides showed that all resolved aromatic signals undergo line broadening ranging from 0.8 to greater than 3.0 Hz in the presence of complex (Table 2) indicating the combination of increasing peptide length and sulfation of Tyr3, Tyr10, and Tyr14 enhances binding to gp120.

2.3. Synthesis of polyethylene glycol-containing alpha amino acid

To determine whether a triply sulfonated peptide also would show increased binding to complex, we synthesized CCR5 Nt ana-

log **8** where TYISN residues were present at positions 3, 10, and 14. Despite containing three sulfonate residues, analog **8** was only sparingly soluble in water hindering extensive binding studies. To overcome this solubility problem, we sought to design and synthesize an alpha amino acid that would be compatible with the conditions used during peptide synthesis, and incorporate both an ethylene glycol side chain and an orthogonal functional group amenable to late-stage chemical modifications (such as Huisgen cycloaddition^{14,15} or Staudinger ligation^{16,17} reactions). Azidation of commercially available chlorohydrin **9** provided the desired masked amino moiety.¹⁸ Bromination of the azido alcohol gave quantitatively the azido bromide,¹⁹ that was used directly to *O*-alkylate Boc-L-serine²⁰ to give *N*-protected azido tris(ethylenoxy) L-alanine **10** (Boc L-ate-Ala).²¹ This 3-step sequence of reactions thus allowed synthesis of multigram quantities of an unnatural amino acid suitable for peptide synthesis using Boc chemistry (see Scheme 1).

Alternatively, TFA deprotection of **10** followed by treatment with FmocCl afforded **11** for use in Fmoc-based solid phase synthesis. For the purpose of immobilization, it was desirable to introduce the PEG amino acid anchor in a position equivalent to CCR5 transmembrane helix 1 (TM1). Thus, the synthesis of a second generation CCR5 TYISN analog **12** was initiated with **11** at the C-terminus. Inclusion of one L-ate-Ala residue increased water solubility of triply sulfonated peptides by greater than 50-fold allowing for preparations of stock solutions exceeding 30 mM compared to a



Scheme 1. Synthesis of the alpha amino acid azido tris(ethylenoxy) *L*-alanine (*L*-ate-Ala). (a) NaN₃, DMF, quant (b) PBr₃, THF, 85% (c) *N*-Boc-*L*-Ser, NaH, DMF, 75% (d) TFA, TIS, CH₂Cl₂ (e) FmocCl, DIPEA, H₂O/dioxane, 75% 2 steps (f) SPPS (g) H₂, Pd/C (h) Cu(II)SO₄, Na ascorbate, propargyl biotin, H₂O/MeOH.

maximum solubility of 0.4 mM observed for peptide **8**. To further demonstrate the utility of the *L*-ate-Ala linker, [2 + 3] Huisgen cyclization of propargyl biotin onto analog **12** readily provided **14** for immobilization or labeling. For the sequence of CCR5 Nt, access to this modification proved especially useful as attempts to biotinylate amine **13** by direct coupling to NHS-biotin resulted in near quantitative intramolecular cyclization between Glu18 and the amine of *L*-ate-Ala.

2.4. Evaluation of triply sulfonated CCR5 Nt

Once in hand, CCR5 Nt tyrosine sulfonate analogs were evaluated for binding to gp120-CD4 by NMR and SPR. Similar to results for triply sulfated peptide **7**, in the presence of gp120-CD4 line broadening of **14**'s aromatic H_δ and H_ε signals occurred (Fig. 5c). Once again, the strongest STD enhancements corresponded to H_δ and H_ε of TYSN 14 and Tyr15, and in contrast to all other sulfated peptides studied, the H_δ and H_ε resonances of TYS3 of **14** were completely resolved showing an ~50% enhancement relative to Tyr15. In addition, STD enhancements of the aryl sulfonate methylenes were observed for all three sulfonate residues (data not shown) providing further evidence that TYSN functions as a TYS isostere in the context of CCR5 Nt peptides. Last, no enhancements were observed for protons within the biotinylated *L*-ate-Ala resi-

due, demonstrating that addition of this linker as well as biotin do not contribute to binding of **14** to gp120-CD4.

The enhanced binding observed by NMR for longer and triply sulfated or sulfonated CCR5 Nt peptides was corroborated by SPR. To assess binding of Nt peptides to gp120-CD4, CD4 was first immobilized onto a carboxymethylated dextran surface. Prior to each injection of Nt peptide, HIV-1 gp120 was introduced to the CD4 surface to assure generation of fresh complex. As seen in Figure 6a, CCR5 Nt peptide **1** bound gp120-CD4 in a concentration dependent manner and in fast exchange with sensorgrams characteristic of fast association and fast dissociation. Steady-state analysis of the binding curves of **1** using Michaelis-Menten kinetics provided an equilibrium dissociation constant of $17 \pm 2 \mu\text{M}$. Triply sulfated CCR5 Nt analog **12** exhibited a vastly different kinetic profile. As seen in Figure 5b, relative to **1** association and dissociation of **12** to gp120-CD4 is slower, and a higher level of late-stage binding is observed. Least squares best fitting of these binding curves to a 1:1 Langmuir binding kinetic model gave an equilibrium dissociation constant of $1.9 \pm 0.02 \mu\text{M}$ for sulfonated peptide **12**. These SPR data were consistent with the variations in binding profiles seen in our NMR experiments where 17- and 19-residue triply sulfated and sulfonated Nt peptides exhibited greater line broadening than the various 14-residue peptides.

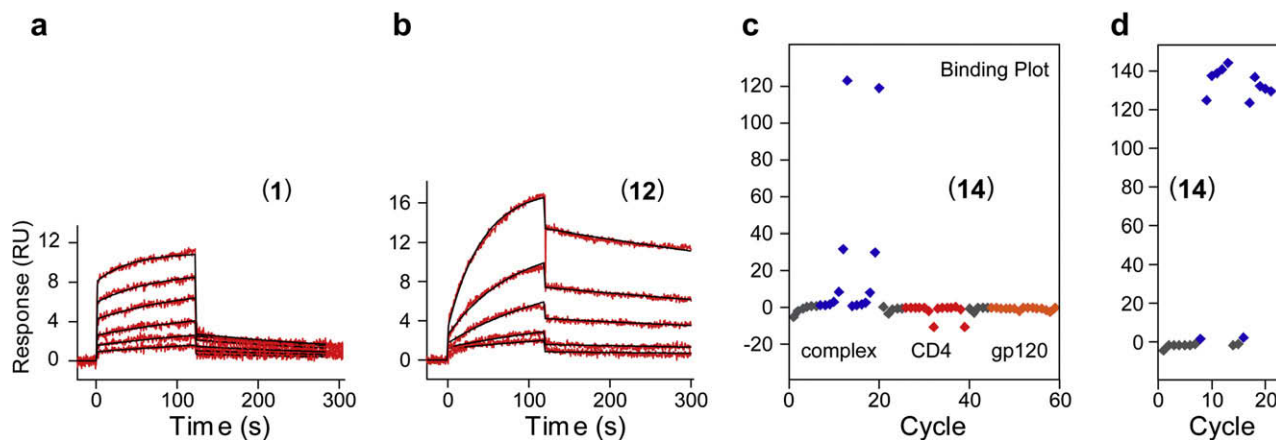


Figure 6. Surface plasmon resonance experiments of CCR5 Nt peptides binding to gp120-CD4. Doubly referenced sensorgrams for (a) doubly sulfated Nt peptide **1** and (b) triply sulfated Nt peptide **12** binding to CD4-captured HIV-1 gp120 with peptide concentrations ranging from 50 to 3.1 μM (twofold serial dilutions). Maximum response (R_{max}) plots for immobilized peptide **14** binding to (c) gp120-CD4 (blue, left), CD4 (red, center), and gp120 (orange, right); and (d) gp120-CD4 in the presence of varying concentrations of mAb 412 d. Protein concentrations in 6 c ranged from 50 to 1.6 μM (twofold serial dilutions), and solutions containing 1 μM gp120-CD4 in the presence of 100–0.001 nM 412 d were used in 6 d. Response units (RUs) are shown on the y-axis with doubly referenced sensorgrams plotted on the same scale for panels (a) and (b). R_{max} points in panels (c) and (d) represent the maximum steady state response observed for each concentration of protein and/or antibody used.

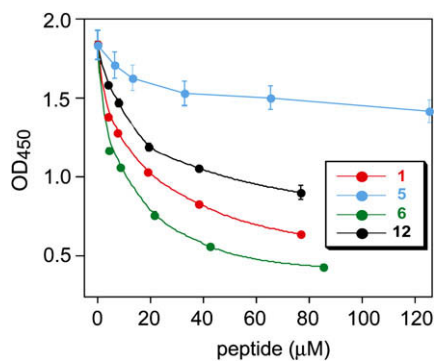


Figure 7. ELISA data showing inhibition of binding of gp120–CD4 to immobilized **14** by sulfated, sulfonated and phosphorylated Nt peptides.

2.5. Development of screening assays using sulfonate isostere **14**

The discovery that the CD4-bound conformation of gp120 possesses a highly conserved sulfo-tyrosine binding pocket potentially presents a new target for HIV-1 Entry inhibitors.⁷ For the purposes of rapid screening and identification of compounds that might inhibit binding of CCR5 to the gp120 TYS binding site, we employed our functional, chemically stable, biotinylated Nt analog **14** to develop rapid screening assays using SPR and ELISA platforms. To test the plausibility of screening by SPR, **14** was immobilized onto a streptavidin-coated chip²² and analyzed for binding to soluble proteins. As shown in the plot of maximum response units (R_{\max}) as a function of varying protein concentrations (Fig. 6c), immobilized **14** bound neither CD4 (red) nor gp120 (orange) on their own, but showed concentration dependent binding to the complex of gp120–CD4 (blue). Both CCR5 Nt and sulfated antibody 412d bind CD4-activated gp120 at the same site at the base of gp120's third variable loop. Consistent with this mode of binding, mAb 412d was able to compete with binding of **14** to CD4-activated gp120 in a dose dependent manner (Fig. 6d). Peptide **14** was further employed to develop an enzyme-linked immunosorbent assay (ELISA) using soluble gp120 and CD4 with colorimetric detection using horseradish peroxidase. Dose dependent binding of gp120–CD4 to immobilized **14** was confirmed, and binding to this complex was inhibited by mAb 412d (plot not shown). To validate the use of this assay for screening of inhibitors, the effect of several sulfated, sulfonated and phosphorylated peptides was assessed. As seen in Figure 7, doubly sulfated peptides **6** and **1** were the strongest inhibitors of **14** binding to gp120 followed by triply sulfonated peptide **12**, and phosphorylated peptide **5** was non-inhibitory.

2.6. Conclusion

In summary, we have analyzed by ¹H NMR, STD NMR and SPR a series of 14-, 17- and 19-residue CCR5 Nt peptides containing variations such as site specific introduction of Tyr(PO₃) and Tyr(SO₄) residues, and two versus three Tyr(SO₄) or Tyr(CH₂SO₃) residues. Results from these studies demonstrated that tyrosine sulfonate can function as a sulfo-tyrosine isostere, allowing us to construct a non-hydrolyzable, sulfonated CCR5 Nt peptide that was used to screen for inhibitors to the CCR5 Nt sulfo-tyrosine binding site on gp120. In addition to increased stability, incorporation of an unnatural amino acid bearing an azido moiety and a tri-ethylene glycol segment (*ate*-Ala) increased solubility of these peptides to levels approaching 100 mg per mL. The orthogonal azido group facilitated late-stage biotinylation through [2 + 3] Huisgen cyclization without side reactions from the other functionalities. We anticipate that sulfonated, chemically stable CCR5 Nt peptide ana-

logs such as **14** will enable the rapid discovery of small molecule inhibitors of HIV-1 gp120 and CCR5 interactions.

3. Experimental

3.1. General

All reactions were performed under a positive flow of nitrogen in flasks that were flame dried under vacuum. Aldrich SureSeal[®] anhydrous solvents (CH₂Cl₂ and DMF) and NMP were used without further purification and stored under nitrogen. Glass-backed TLC plates (EMD Silica Gel 60 with a 254 nm fluorescent indicator) were cut into 2 × 5 cm portions and stored over desiccant. Developed TLC plates were visualized at 254 nm, stained with an I₂-SiO₂ mixture, and/or treated with Hanessian's stain or PMA and charred. Column chromatography was conducted using a Biotage Sp4 automated purification system and fractions collected by monitoring at 254 nm. NMR experiments (1D and 2D) were conducted on Varian Gemini 300 and Bruker AVANCE 500 and 600 MHz spectrometers using specified solvents at 298 K. FT-IR data were acquired using a Perkin Elmer ATR-FTIR attachment. All Fmoc amino acids, resins, and coupling reagents used for peptide synthesis were purchased from Peptides International; and peptides **1–3** and **5** were purchased from American Peptide Company. Figures were made using the programs Pymol²³ and LigPlot.²⁴

3.2. Reagents and conditions for NMR experiments

Peptides were dissolved in freshly prepared and sterile filtered "NMR Buffer" (20 mM sodium phosphate, 50 mM NaCl, pH 6.8), and peptide stock solutions were adjusted to pH 6.8. Soluble CD4 (two-domain) was obtained from the AIDS Research and Reference Reagent Program (Cat. No. 4615: Progenics Pharmaceuticals). YU2 gp120, with a Gly-Ala-Gly tripeptide replacing the V1/V2 region, was produced by a *Drosophila* Schneider 2 line under control of an inducible metallothionein promoter²⁵ and purified by affinity chromatography as described previously.²⁶ All proteins and protein complexes were passed through a Superdex 200 16/60 gel filtration column in NMR Buffer, and quantified by A₂₈₀ measurements prior to use. Typical NMR samples contained 800 μM peptide with or without 20 μM protein (270 μL + 30 μL D₂O). ¹H, ¹³C, and ¹⁵N NMR assignments were made using data from 2D HOHAHA, ROESY, ¹H-¹³C HSQC, ¹H-¹³C HSQC-TOCSY, and ¹H-¹H ROESY experiments recorded at 298 K using standard Bruker pulse programs with water suppression. (Complete resonance assignments are provided in the Supporting Information.) Saturation transfer difference (STD) NMR experiments were recorded with the carrier set at -1 or 12 ppm for on-resonance irradiation and 50 ppm for off-resonance irradiation. Selective protein saturation (duration ranging from 1 to 5 s) was accomplished using a train of 50 ms Gauss-shaped pulses, each separated by a 1 ms delay, at an experimentally determined optimal power (49 dB on our probe); a T1ρ filter (30 ms) was incorporated to suppress protein resonances. A minimum of 512 scans and 4000 points were used to ensure high quality data with good signal-to-noise. On- and off-resonance spectra were processed independently, and subtracted to provide a difference spectrum. For all complexes, the signal corresponding to 15ε was most strongly enhanced; thus spectra were normalized to this signal.

3.3. Production of 412d-antigen-binding fragment (Fab)

Monoclonal antibody 412d was purified from mouse-human hybridomas by staphylococcal protein A chromatography. 412d Fab was generated by endoproteinase Lys-C digestion of the 412d IgG and purified as described previously.²⁷ Briefly, the 412d antibody was cleaved by Lys-C protease (Roche) to produce Fab, with

affinity (Protein A), size-exclusion (Superdex S200), and anion-exchange (Mono-Q) chromatography used to separate the most cationic (double-sulfated) fragment.

3.4. Surface plasmon resonance

Surface plasmon resonance experiments were performed using a Biacore T100 instrument and accompanying software. Following optimization by pH scouting, CD4 (0.5 M in 20 mM acetate, pH 5.5) was immobilized on a CM5 chip with HBS-EP as immobilization buffer to a response level of 500 RUs, and remaining activated surface was capped with 1 M ethanolamine (pH 8.0). Immobilization buffer was replaced and the chip equilibrated with PBS as the running buffer for binding and kinetics analyses.

For analyses of peptides' binding to immobilized protein, solutions of CCR5 Nt peptides were prepared in PBS at concentrations of 30–50 mM, and appropriate twofold serial dilutions were employed for binding studies. After capture of soluble HIV-1 gp120 (YU2 strain, 1 μ M in PBS) onto the CD4 flow cell (FC) to a response of 2000 RUs, peptide solutions were injected with association and dissociation times of 120 and 180 s, respectively. Binding analyses were performed at 25 °C at a flow rate of 30 μ L/min using serially arranged control (FC1) and active flow (FC2) cells. The CD4 surface was regenerated using a short pulse (8 s) of regeneration solution (50 mM NaOH, 1 M NaCl) at a flow rate of 60 μ L/min. Using the T100 BiaEvaluation software, all data were doubly referenced to control flow cell and zero concentration data curves prior to curve fitting using a 1:1 binding model.

To analyze proteins and complexes binding to immobilized peptides, a Biacore SA (streptavidin) chip was docked onto a Biacore T100 with PBS as the running buffer at 5 μ L/min. All flow cells (FCs) were conditioned with injections (3×60 s) of 50 mM NaOH, 1 M NaCl. Biotinylated peptide **14** (50 nM in PBS) was immobilized onto FC2 to a response level of \sim 300 RUs. All proteins samples were purified on a Superdex 200 16/60 gel filtration column in PBS, and quantified by A_{280} measurements prior to use. Serially diluted solutions of proteins in PBS (gp120, CD4, CD4–gp120 complex) were prepared and injected sequentially through FC1 and FC2. All protein binding analyses were performed at 25 °C at a flow rate of 20 μ L/min. Regeneration of the surface was achieved with a short pulse (8 s) of 50 mM NaOH, 1 M NaCl using a flow rate of 60 μ L/min. Data were processed using T100 BiaEvaluation software where data from the control flow cell (FC1) was subtracted from the binding/peptide flow cell (FC2). These binding curves were referenced to a negative control (buffer injection) giving double referenced binding data.

3.5. CCR5 Nt peptide ELISAs

Neutravidin-coated high binding capacity, pre-blocked ELISA plates (Pierce) were washed three times with assay buffer (Dulbecco's phosphate buffered saline, 0.05% P20, 1% fetal bovine serum, and 2% bovine serum albumin). Plates were incubated with biotinylated CCR5 Nt peptide **14** (500 nM) for 1 h at rt, then washed three times with assay buffer. A complex made of 60 nM YU2 Δ V1V2 gp120, 120 nM sCD4 and 60 nM 2.2c IgG in assay buffer was incubated for 1 h with or without addition of inhibitor (either a CCR5 Nt analog or 412 d IgG). Antibody 2.2c is an A32-like antibody that binds to the C1–C4 region of monomeric gp120 (James Robinson, personal communication). The complex was then added to an ELISA plate with immobilized **14** and incubated for 1 h. Plates were washed three times with assay buffer, and HRP-conjugated goat anti-human IgG was used to detect the presence of bound gp120–CD4–2.2c IgG complex. The plates were developed using the TMB Peroxidase EIA Substrate Kit (Bio-Rad).

3.6. N-Boc azido tris-(ethylenoxy) L-alanine (**10**)

To a cooled, 0 °C, solution of Boc L-Ser (29.7 g, 145 mmol) in DMF (400 mL) was added NaH (12.8 g, 319 mmol, 60% dispersion in mineral oil). The cloudy suspension was allowed to stir for an additional 15 min at rt. Azido bromo PEG¹⁴ (23.0 g, 96.6 mmol) in DMF (100 mL) was added dropwise and the mixture was stirred overnight, 15 h. The solution was concentrated in vacuo and purified by Si gel chromatography (10% MeOH/CH₂Cl₂) to afford **10** (26.0 g, 75% yield). ¹H NMR (CD₃OD, 300 MHz) δ 4.27 (br, 1 H), 3.88 (dd, 1H, J = 4.5 Hz, 9.3 Hz), 3.74 (d, 1H, J = 3.3 Hz), 3.66 (m, 8H), 3.38 (t, 2H, J = 4.8 Hz), 1.45 (s, 11H). ¹³C NMR (CD₃OD, 75 MHz) δ 158.1, 101.9, 80.8, 80.0, 72.1, 71.9, 71.8, 71.6, 71.3, 51.9, 28.6. ATR-FTIR (cm⁻¹): 3697, 2974, 2923, 2871, 2104, 1709, 1393, 1367, 1165, 1119, 1056, 1033. HRMS (TOF-MS-ES) m/z 361.1696, (361.1723 Calcd for C₁₄H₂₆N₄O₇, M-H).

3.7. N-Fluorenylmethylcarbonyl azido tris-(ethylenoxy) L-alanine (**11**)

N-Boc-protected amino acid **10** (1.4 g, 3.9 mmol) was dissolved in CH₂Cl₂ (10 mL) and cooled to 0 °C. Following the addition of triisopropylsilane (0.8 mL, 3.9 mmol), trifluoroacetic acid (2 mL) was syringed into the stirring mixture. The reaction was allowed to warm to rt overnight (15 h) and concentrated to dryness in vacuo. TOF-MS-ES revealed complete conversion to free amino acid [HRMS-ESI m/z 261.1206 [M-H] (C₉H₁₇N₄O₅ calculated 261.1199)] which was dissolved in H₂O:dioxane (10:10 mL) and adjusted to pH 8 with DIPEA (2.5 mL, 15 mmol). To the cooled mixture (0 °C) was added a solution of FmocCl (1.2 g, 4.7 mmol) in dioxane (5 mL). The solution was allowed to warm to rt overnight (16 h) and concentrated to dryness in vacuo. The crude mixture was purified using silica gel column chromatography with a gradient of 5–10% MeOH:CH₂Cl₂ over 10 column volumes to provide **11** (1.26 g, 67% over 2 steps). ¹H NMR (DMSO-*d*₆, 300 MHz) δ 7.89 (d, 2H, J = 7.5 Hz), 7.73 (d, 2H, J = 7.2 Hz), 7.42 (t, 2H, J = 7.2 Hz), 7.32 (t, 2H, J = 7.5 Hz), 4.26 (m, 3H), 4.09 (m, 1H), 3.68 (d, 1H, J = 4.8 Hz), 3.57 (t, 2H, J = 4.8 Hz), 3.55 (t, 2H, J = 5.1 Hz), 3.52 (s, 4H, 2.07), 3.38 (t, 2H, J = 6.3 Hz), 3.36 (t, 2H, J = 4.8 Hz), 1.12 (t, 2H, J = 7.2 Hz). ¹H NMR (CD₃OD, 300 MHz) δ 7.90 (d, 2H, J = 6.9 Hz), 7.79 (t, 2H, J = 6.2 Hz), 7.49 (t, 2H, J = 7.5 Hz), 7.42 (dt, 2H, J = 1.2 Hz, 7.5 Hz), 4.46 (d, 2H, J = 6.3 Hz), 4.34 (m, 2H), 3.96 (dd, 1H, J = 5.6 Hz, 9.8 Hz), 3.87 (dd, 1H, J = 5.6 Hz, 9.8 Hz), 3.72 (m, 8H), 3.43 (m, 2H), 1.00 (t, 2H, J = 3.9 Hz). ¹³C NMR (DMSO-*d*₆, 75 MHz) δ 171.9, 155.9, 143.9, 140.7, 127.6, 127.1, 125.3, 120.1, 70.4, 69.7, 69.6, 69.3, 65.7, 60.4, 54.9, 50.0, 48.6, 46.7, 45.1, 40.3. ATR-FTIR (cm⁻¹) 3310, 3066, 2884, 2105, 1717, 1450. HRMS (TOF-MS-ES) m/z 485.2041 (485.2036 Calcd for C₂₄H₂₉N₄O₇, M+H).

3.8. Solid phase peptide synthesis of CCR5 Nt TYSN analog **12**

CLEARTM amide resin was swelled in NMP for 10 min with gentle agitation by a flow of dry N₂ (g) and washed with copious amounts of CH₂Cl₂ and NMP. Removal of the Fmoc protecting group was accomplished through treatment with 20% piperidine for 20 min. Following deprotection, the resin was washed with CH₂Cl₂, MeOH, and NMP successively prior to coupling of a subsequent amino acid. Each coupling step required exposure of the resin with 4 equiv each of Fmoc amino acid, PyBOP, and DIPEA for 2–4 h. Each coupling was followed by wash cycles of CH₂Cl₂ and MeOH followed by acetylation with 20% Ac₂O in CH₂Cl₂ for 20 min. A double coupling using Fmoc-TYSN was required for TYS3 and TYS10. Treatment of the cooled resin with TFA/H₂O/TIS (95:2.5:2.5) at 4 °C for 2 h effectively cleaved the peptide from the resin with concomitant global deprotection, after which the peptide was precipitated by addition of cold MTBE (5 \times volume of TFA). Peptides were

purified using RP-HPLC with a YMC-Pack ODS-AQ column using 10 mM NH_4CHO_2 and MeOH as eluents. Lyophilization provided **12** as a white powder. ^1H NMR (D_2O , 500 MHz) δ 7.27 (d, 2H, $J = 7.7$ Hz), 7.23 (d, 2H, $J = 7.7$ Hz), 7.20 (d, 2H, $J = 7.7$ Hz), 7.13 (t, 4H, $J = 7.7$ Hz), 7.05 (d, 2H, $J = 8.2$ Hz), 6.94 (d, 2H, $J = 7.7$ Hz), 6.75 (d, 2H, $J = 8.2$ Hz), 4.55 (m, 1H), 4.40 (m, 2H), 4.34–4.23 (m, 5H), 4.14 (m, 2H), 4.08–3.93 (m, 17H), 3.88 (d, 4H, $J = 5.9$ Hz), 3.84–3.68 (m, 21H), 3.59 (br s, 21H), 3.39 (t, 2H, $J = 4.7$ Hz), 3.11–3.00 (m, 4H), 2.93–2.90 (m, 6H), 2.79 (dd, 1H, $J = 6.9$ Hz, 17 Hz), 2.68–2.50 (m, 6H), 2.35 (t, 3H, $J = 8.1$ Hz), 2.18 (t, 2H, $J = 7.6$ Hz), 2.11–1.87 (m, 14H), 1.76 (m, 1H), 1.70–1.64 (m, 3H), 1.33 (m, 4H), 1.11 (br d, 7H, $J = 6.2$ Hz), 1.01 (m, 2H), 0.86 (d, 10H, $J = 6.7$ Hz), 0.79 (t, 6H, $J = 7.3$ Hz), 0.75–0.70 (m, 8H), 0.66 (d, 3H, $J = 6.7$ Hz). ^{13}C NMR (D_2O , 150 MHz) δ 178.53, 178.32, 178.25, 174.89, 174.73, 174.51, 174.16, 174.07, 173.99, 173.92, 173.61, 173.52, 173.40, 173.28, 173.14, 172.59, 172.53, 172.01, 169.20, 155.25, 136.55, 136.43, 131.26, 130.02, 129.90, 129.83, 129.21, 128.81, 128.11, 126.15, 125.95, 125.11, 118.21, 117.60, 116.25, 115.17, 114.31, 111.35, 110.51, 107.39, 105.36, 102.91, 102.68, 100.77, 100.70, 100.64, 98.01, 70.77, 70.32, 70.26, 70.22, 69.91, 67.72, 64.39, 61.78, 61.55, 61.35, 60.15, 59.80, 59.30, 57.23, 56.61, 56.25, 56.01, 55.24, 54.26, 54.15, 54.05, 53.64, 51.55, 51.13, 50.98, 50.86, 48.80, 43.21, 37.35, 37.06, 36.65, 31.68, 31.16, 30.87, 30.03, 27.42, 26.87, 25.48, 25.32, 22.44, 19.39, 19.12, 18.37, 15.47, 15.43, 11.26, 10.45. HRMS (TOF-MS-ES) m/z 2633.0002 [M+H], 1315.9836 [M–2H], 876.6529 [M–3H], (2633.0006 Calcd for $\text{C}_{109}\text{H}_{158}\text{N}_{25}\text{O}_{45}\text{S}_3$ [M+H]).

3.9. Reduction of **12** to amine **13**

Azide **12** (10 mg, 3.8 μmol) was dissolved in MeOH/ H_2O /HOAc (1:4:0.1, 5 mL) and Pd/C (5 mg) was added. The flask was evacuated and charged with H_2 (g); this was repeated twice. The mixture was stirred under H_2 (g) at atmospheric pressure for 2 h after which the Pd/C was removed by filtering through a pad of Celite and the solvent removed in vacuo. HRMS data revealed complete reduction of azide **12** to amine **13**. HRMS (TOF-MS-ES) m/z 1302.4938 [M–2H], 867.9971 [M–3H] (calcd for $\text{C}_{109}\text{H}_{160}\text{N}_{23}\text{O}_{45}\text{S}_3$ [M–H] 2604.9944).

3.10. Synthesis of biotin conjugated **14**

To a solution of azide **12** (14.7 mg, 5.6 μmol) in PBS/*tert*-butyl alcohol (1:1, v/v, 700 μL) were added CuSO_4 (50 mM, 4 μL), sodium ascorbate (100 mM, 180 μL), and propargyl biotin (5.0 mg, 18 μmol) and the mixture was stirred overnight at rt. Complete conversion to conjugate **14** was verified by LCMS; MS (ES) m/z 1457.5 [M–2H], 970.5 [M–3H] (2915.12 Calcd for $\text{C}_{122}\text{H}_{176}\text{N}_{28}\text{O}_{47}\text{S}_4$, M). Purification was accomplished using RP-HPLC using a Waters Symmetry-Prep C8 column with 20 mM NH_4CHO_2 and CH_3CN as mobile phases. Lyophilization gave **14** as white powder. Complete ^1H and ^{13}C NMR assignments are provided in the Supporting Information.

Acknowledgments

We thank J. Lloyd for HRMS data, J. Robinson for 412d and 2.2c antibodies, C.-C. Huang for assistance with expression and purifica-

tion of gp120 and antibodies, and the NIH AIDS Research and Reference Regent Program for soluble CD4. This work was supported by the NIDDK (C.A.B.) and NIAID (P.D.K. and R.W.) Intramural Research Programs, a grant from the Bill and Melinda Gates Foundation Grand Challenges in Global Health Initiative (P.D.K. and R.W.), and the Intramural AIDS Targeted Antiviral Program (IATAP) of the Office of the Director, NIH (C.A.B.).

Supplementary data

Spectral data for protected amino acids **10** and **11**, peptides **12** and **13**, and complete ^1H and ^{13}C assignments for peptides **2–4**, **6**, **7** and **14**. Supplementary data associated with this article can be found, in the online version, at doi:10.1016/j.bmc.2008.10.005.

References and notes

- Wyatt, R.; Sodroski, J. *Science* **1998**, *280*, 1884–1888.
- Berger, E. A.; Murphy, P. M.; Farber, J. M. *Annu. Rev. Immunol.* **1999**, *17*, 657–700.
- Farzan, M.; Mirzabekov, T.; Kolchinsky, P.; Wyatt, R.; Cayabyab, M.; Gerard, N. P.; Sodroski, J.; Choe, H. *Cell* **1999**, *96*, 667–676.
- Farzan, M.; Chung, S.; Li, W.; Vasilieva, N.; Wright, P. L.; Schnitzler, C. E.; Marchione, R. J.; Gerard, C.; Gerard, N. P.; Sodroski, J.; Choe, H. *J. Biol. Chem.* **2002**, *277*, 40397.
- Cormier, E. G.; Persuh, M.; Thompson, D. A. D.; Lin, S. W.; Sakmar, T. P.; Olson, W. C.; Dragic, T. *Proc. Natl. Acad. Sci.* **2000**, *97*, 5762–5767.
- Farzan, M.; Vasilieva, N.; Schnitzler, C. E.; Chung, S.; Robinson, J.; Gerard, C.; Choe, H.; Sodroski, J. *J. Biol. Chem.* **2000**, *275*, 33516–33521.
- Huang, C.-C.; Lam, S. N.; Acharya, P.; Shahzad-ul-Hussan, S.; Stanfield, R. L.; Tang, M.; Xiang, S.-H.; Robinson, J.; Sodroski, J.; Wilson, I.; Wyatt, R.; Bewley, C. A.; Kwong, P. D. *Science* **2007**, *317*, 1930–1934.
- Kitagawa, K.; Aida, C.; Fujiwara, H.; Yagami, T.; Futaki, S.; Kogire, M.; Ida, J.; Inoue, K. *J. Org. Chem.* **2002**, *66*, 1–10.
- Mayer, M.; Meyer, B. *Angew. Chem. Int. Ed.* **1999**, *38*, 1784–1788.
- An alternate explanation may in part be attributed to the absence of a hydrogen bond acceptor (carboxylate) in the TYS binding site should monobasic phosphate be present Quiocho, F. A. *Kidney Int.* **1996**, *49*, 943–946.
- Gonzalez-Muniz, R.; Cornille, F.; Bergeron, F.; Ficheux, D.; Pothier, J.; Durieux, C.; Roques, B. P. *Int. J. Pept. Prot. Res.* **1991**, *37*, 331–340.
- Miranda, M. T. M.; Liddle, R. A.; Rivier, J. E. *J. Med. Chem.* **1993**, *36*, 1681–1688.
- Seibert, C.; Cadene, M.; Sanfz, A.; Chait, B. T.; Sakmar, T. P. *Proc. Natl. Acad. Sci. U.S.A.* **2002**, *99*, 11031–11036.
- Kolb, H. C.; Finn, M. G.; Sharpless, K. B. *Angew. Chem. Int. Ed.* **2001**, *40*, 2004–2021.
- For a recent review of reactions involving organic azides Bräse, S.; Gil, C.; Knepper, K.; Zimmermann, V. *Angew. Chem. Int. Ed.* **2005**, *44*, 5188–5240.
- Saxon, E.; Armstrong, J. I.; Bertozzi, C. R. *Org. Lett.* **2000**, *2*, 2141–2143.
- Kohn, M.; Breinbauer, R. *Angew. Chem. Int. Ed.* **2004**, *43*, 3106–3116.
- Iyer, S. S.; Anderson, A. S.; Reed, S.; Swanson, B.; Schmidt, J. G. *Tetrahedron Lett.* **2004**, *45*, 4285–4288.
- Roy, B. C.; Santos, M.; Mallik, S.; Campiglia, A. D. *J. Org. Chem.* **2003**, *68*, 3999–4007.
- Hwang, J.; Deming, T. J. *Biomacromolecules* **2001**, *2*, 17–21.
- An eight step synthesis (overall yield of 11%) of the free amine of **11**, starting from an L-serine derived aziridine followed by nucleophilic ring opening, has been reported Larsson, U.; Carlson, R. *Acta Chem. Scand.* **1994**, *48*, 511–516.
- Attempts to couple amine **13** to a carboxymethyl chip using a variety of conditions such as varying pH and salt concentration were unsuccessful, likely owing to the negative charge of both the peptide and surface.
- <http://pymol.sourceforge.net/>.
- Wallace, A. C.; Laskowski, R. A.; Thornton, J. M. *Prot. Eng.* **1995**, *8*, 127–134.
- Wu, L.; Gerard, N. P.; Wyatt, R.; Choe, H.; Parolin, C.; Ruffing, N.; Borsetti, A.; Cardoso, A. A.; Desjardin, E.; Newman, W.; Gerard, C.; Sodroski, J. *Nature* **1996**, *384*, 179–183.
- Wyatt, R.; Sullivan, N.; Thali, M.; Repke, H.; Ho, D.; Robinson, J.; Posner, M.; Sodroski, J. *J. Virol.* **1993**, *67*, 4557–4565.
- Huang, C.-C.; Venturi, M.; Majeed, S.; Moore, M. J.; Phogat, S.; Zhang, M. Y.; Dimitrov, D. S.; Hendrickson, W. A.; Robinson, J.; Sodroski, J.; Wyatt, R.; Choe, H.; Farzan, M.; Kwong, P. D. *Proc. Natl. Acad. Sci. U.S.A.* **2004**, *101*, 2706–2711.